
Figures and figure supplements

Tailoring T_{fh} profiles enhances antibody persistence to a clade C HIV-1 vaccine in rhesus macaques

Anil Verma and Chase E Hawes *et al.*

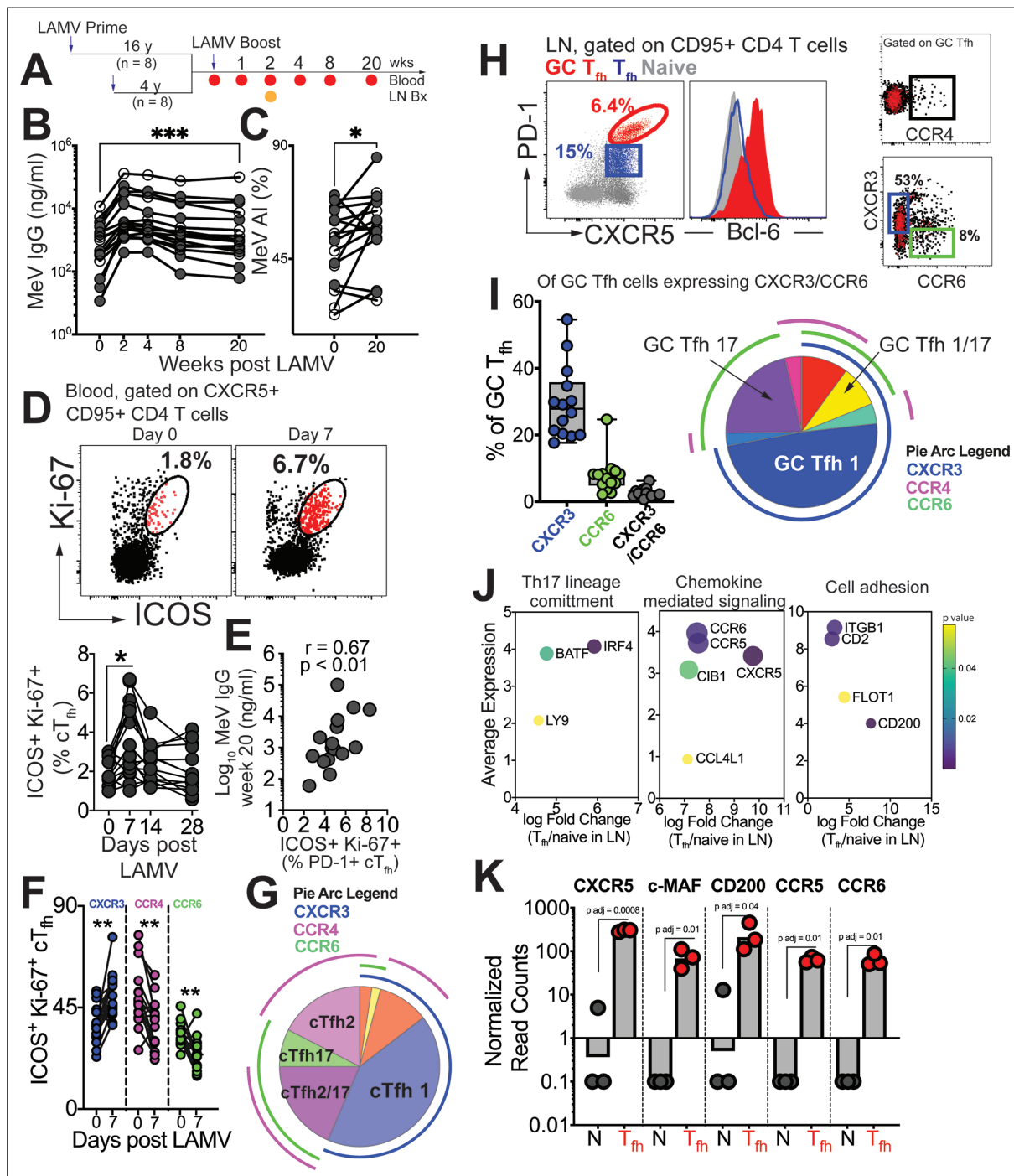


Figure 1. GC T_h1 and GC T_h17 cells recalled by measles booster. (A) Overview of study design; adult female rhesus macaques immunized with Live Attenuated Measles Virus vaccine (LAMV). (B) Serum MeV IgG kinetics measured by ELISA (filled circles, aged rhesus; open circles, young adults). (C) Avidity index (AI) of MeV IgG measured using chaotropic displacement ELISA with sodium thiocyanate at week 20 and week 0 in serum. (D) Representative flow cytometry plots showing ICOS⁺Ki-67⁺ circulating (c)Tfh cells in blood at day 0 and day 7 post LAMV. Kinetics of ICOS⁺Ki-67⁺ cTfh cells. (E) Correlation between ICOS⁺Ki-67⁺ cTfh cells at day 7 and MeV IgG at week 20. (F) T_h profile of cTfh cells shows induction of CXCR3⁺ cTfh1 at day 7. (G) Boolean analysis (n=16) shows cTfh1 cells induced 1 week post LAMV. Overlapping pie arcs denote cTfh cells expressing multiple chemokine receptors as denoted by arc color. (H) Representative flow cytometry plots show CXCR5⁺ PD-1⁺⁺ GC T_h cells and histogram shows Bcl-6 expression on GC T_h cells. T_h profile of GC T_h cells shows expression of CXCR3 and CCR6. (I) Boolean analysis of GC T_h cells expressing either CXCR3 or CCR6 (n=14) shows proportion of T_h1, T_h17 and T_h1/17 GC T_h subsets. (J) Bubble plots show genes for significantly enriched pathways related to T helper differentiation on sorted CXCR5⁺ PD-1⁺⁺ cells. (K) Gene expression on sorted CXCR5⁺ PD-1⁺⁺ cells. Statistical analysis was performed using two-tailed Wilcoxon matched-pairs signed rank test (in panels B-D, F) or spearman rank correlation test (E); * p<0.05, **p<0.01, *** p<0.001, **** p<0.0001.

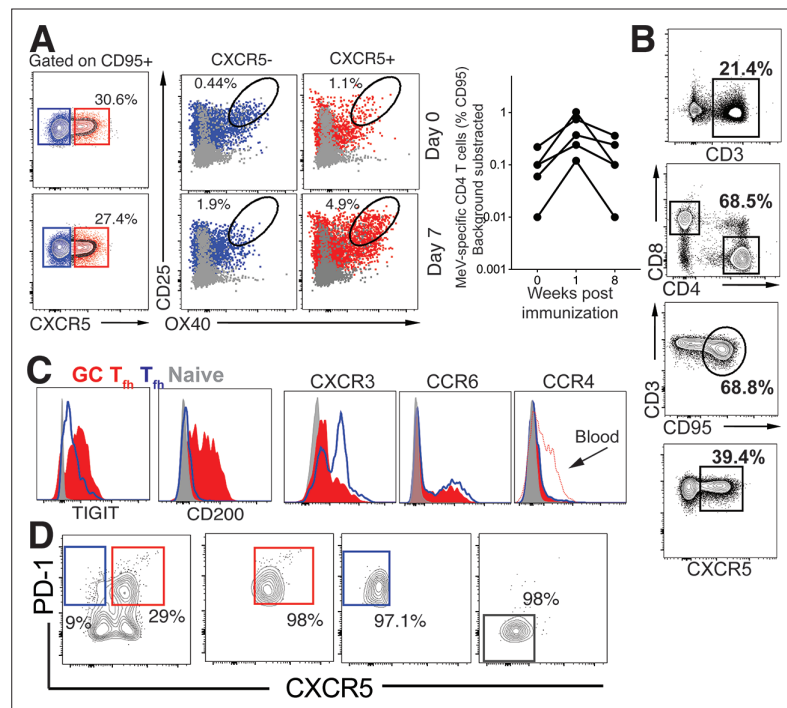


Figure 1—figure supplement 1. MeV specific T_{fh} cells. **(A)** Gating strategy to identify CXCR5⁺ OX40⁺ CD25⁺ MeV-specific T_{fh} cells within PBMCs following stimulation with MeV antigen at Day 0 and Day 7 post LAMV. Right panel illustrates the MeV specific responses in CD4 T cells (%CD95) at weeks 0, 1, and 8 following immunization. **(B)** Flow plots illustrate gating strategy to identify cT_{fh} cells. **(C)** Representative histograms show expression of TIGIT, CD200, CXCR3, CCR6, and CCR4 on GC T_{fh} cells in LN. **(D)** Sorting schematic to isolate CXCR5 + PD-1^{+/++} cells for RNA sequencing.

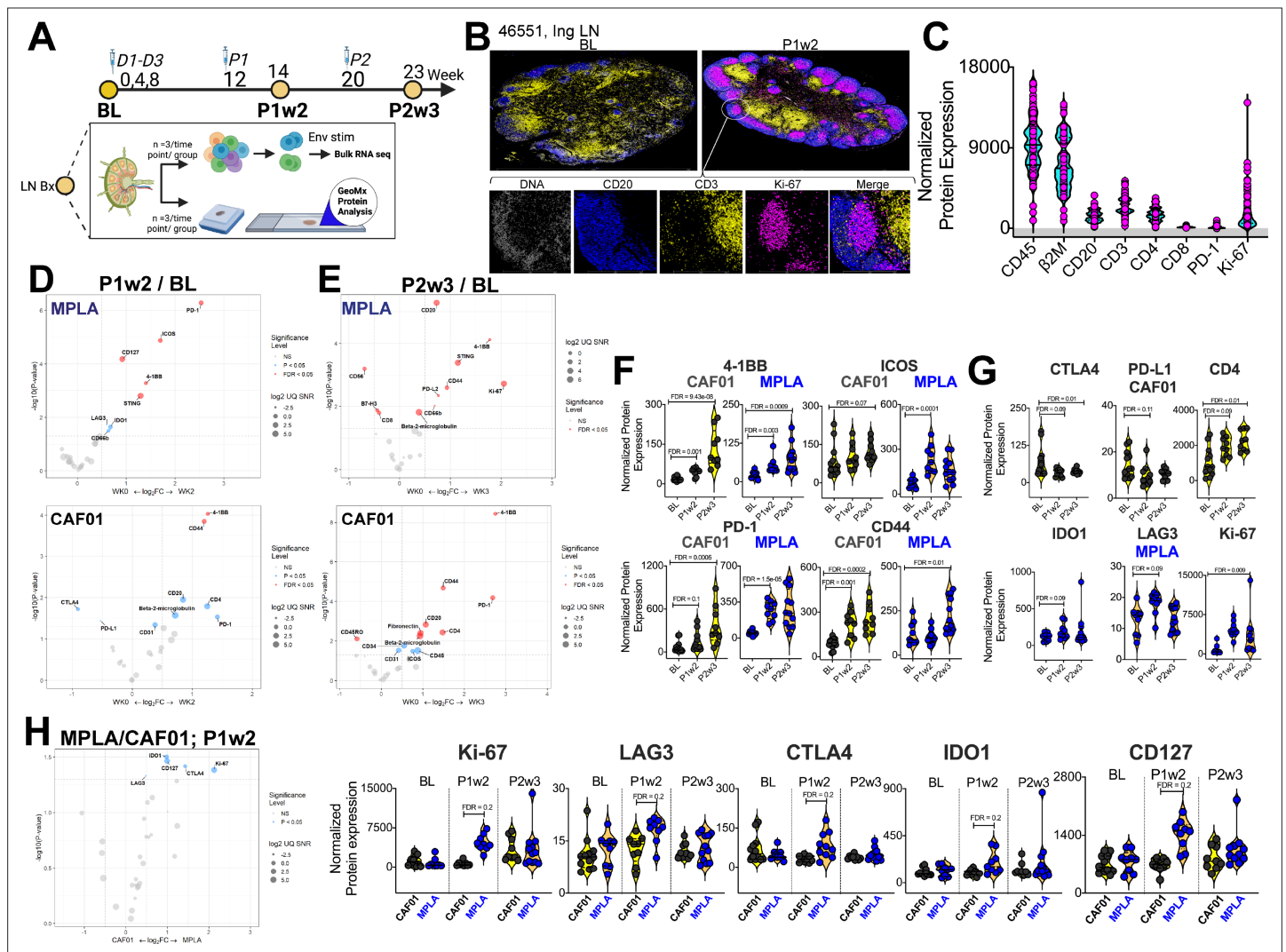


Figure 2. Induction of Robust T Cell Activation in GCs with HIV-1 Env Formulated in CAF01 and MPLA +QS-21 Adjuvants. **(A)** Overview of experimental design for in-situ proteomics and transcriptional analysis. **(B)** Representative images of GC from FFPE sections of inguinal LN at baseline and week 2 post protein 1 immunization with HIV-Env gp140 | MPLA +QS-21; scale bar; top, 3 mm, close up, 300 μ m. LN sections were stained for CD20 (blue), CD3 (yellow), Ki-67 (magenta), and DNA (gray) to identify GCs. Circular ROIs (100 μ m in diameter, total 60) were selected based on co-localization of CD3 with CD20 +Ki-67+GC B cells for proteomic profiling with a 32-plex antibody cocktail. Normalized protein expression (NPE) values were calculated using three negative control IgG probes. **(C)** NPE of key lineage markers across all ROIs at BL, P1w2, and P2w3. **(D-E)** Volcano plots show proteins induced post boost in each vaccine group. **(F)** Violin plots show common proteins induced post protein boost in MPLA and CAF01 groups. **(G)** Violin plots of proteins induced with CAF01 and MPLA. **(H)** Volcano plot (left) and Violin plots (right) of proteins significantly different across HIV-1 Env gp140 MPLA +QS-21 and CAF01 regimens. Differential expression was modeled using a linear mixed-effect model to account for the sampling of multiple ROI/AOI segments per patient/tissue. Criterion of significance was nominal p-value < 0.05 , plots show False discovery rate (FDR).

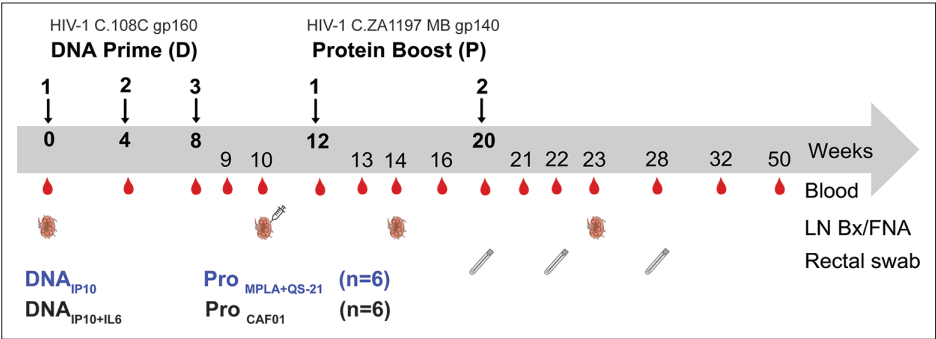


Figure 2—figure supplement 1. Experimental design of DNA-prime/Protein-boost Clade C HIV-1 immunization.

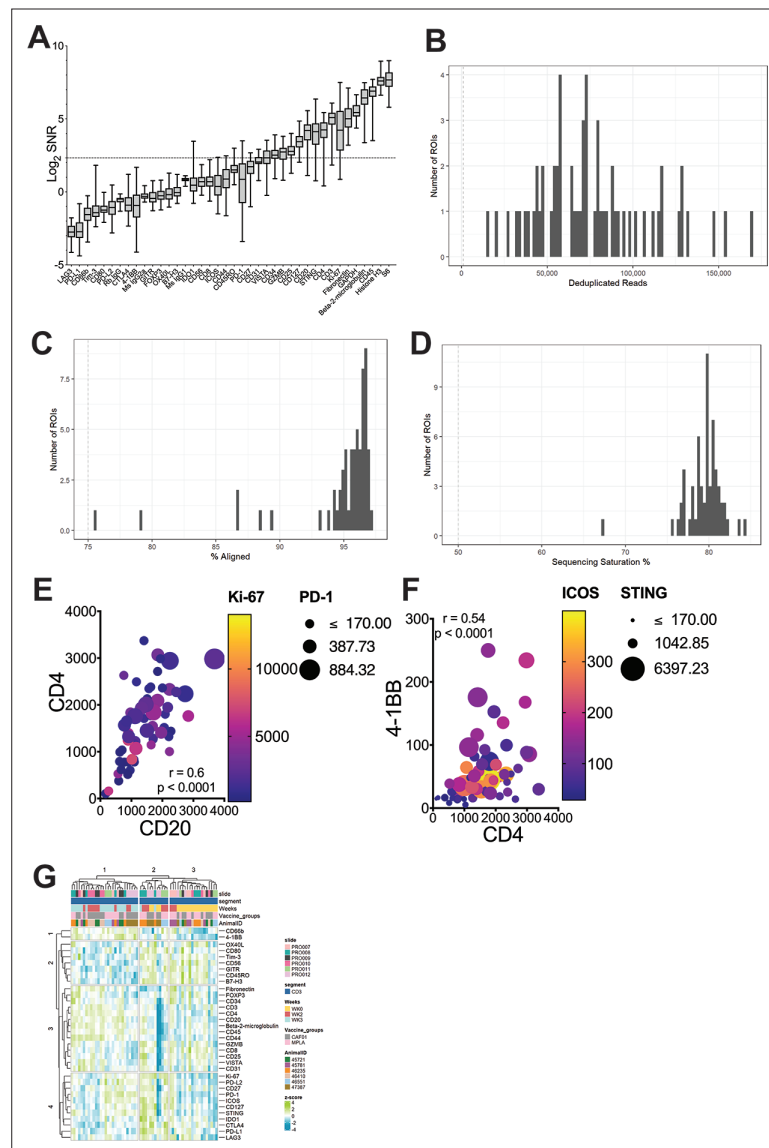


Figure 2—figure supplement 2. Sequencing QC histograms show (A) Signal-to-noise ratio computed by dividing raw count values by the geometric mean of the negative IgG probes. Quality control metrics- (B) deduplicated reads, (C) percent aligned reads, (D) sequencing saturation. (E) Bubble plot shows correlation of CD20 protein expression with CD4; bubble size corresponds to PD-1 expression, color intensity, Ki-67 expression; Spearman value, two-tailed p value of 60 pairs. (F) Bubble plot shows correlation of CD4 protein expression with 4-1BB; bubble size corresponds to ICOS expression, color intensity, STING expression; Spearman value, two-tailed p value of 60 pairs. (G) Heatmap plots show unsupervised hierarchical clustering of z-score values for each protein across time for each animal.

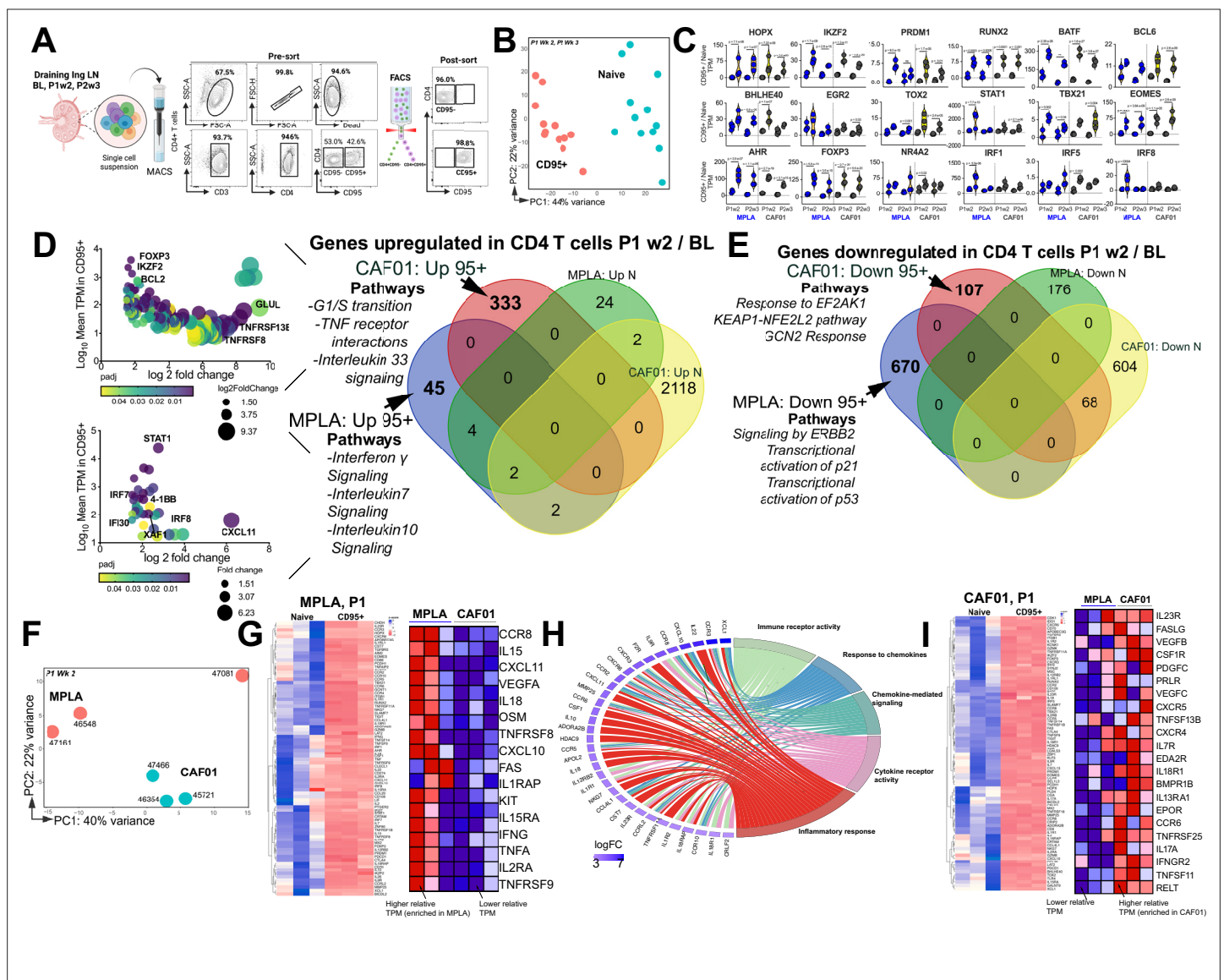


Figure 3. T_H1 molecular programs potentiated by HIV-1 Env/MPLA + QS-21. **(A)** FACS purified CD95⁻ (naive [N]) and CD95⁺ CD4 T cells, stimulated overnight with HIV-1 Env, were sequenced to assess transcriptional programs. **(B)** Principal component analysis (PCA) of all expressed genes shows distinct clustering of N and CD95⁺ cells. **(C)** Violin plots show transcripts per million (TPM) values of differentially expressed transcription factors (p adj < 0.05) in CD95⁺ CD4 T cells relative to naive CD4 T cells post vaccination. **(D)** Bubble plots depict DEG at P1w2 versus BL in CD95⁺ CD4 T cells in CAF01 (top) and MPLA (bottom). Venn Diagram of DEG genes upregulated in CD95⁺ and naive subsets at P1w2 relative to BL shows 45 and 333 genes exclusively upregulated in CD95⁺ CD4 T cells with MPLA and CAF01, respectively. **(E)** Venn diagram of significantly downregulated genes. **(F)** PCA of all expressed genes shows distinct clustering across vaccine groups at P1w2. **(G)** Heat maps depict log₂ gene expression (transcripts per million (TPM)) for highly DEG in CD95⁺ cells compared to naive cells at P1w2 in MPLA; heat map in inset depicts TPM of genes represented in Cytokine-cytokine receptor interaction pathways across vaccine regimens. **(H)** Chord plot shows GO Terms enriched with corresponding upregulated genes in CD95⁺ CD4 T cells at P1w2 with MPLA. **(I)** Heat maps depict log₂ gene expression (TPM) for highly DEG in CD95⁺ cells compared to naive cells at P1w2 in CAF01; heat map in inset depicts TPM of genes represented in Cytokine-cytokine receptor interaction pathway across vaccine regimens.

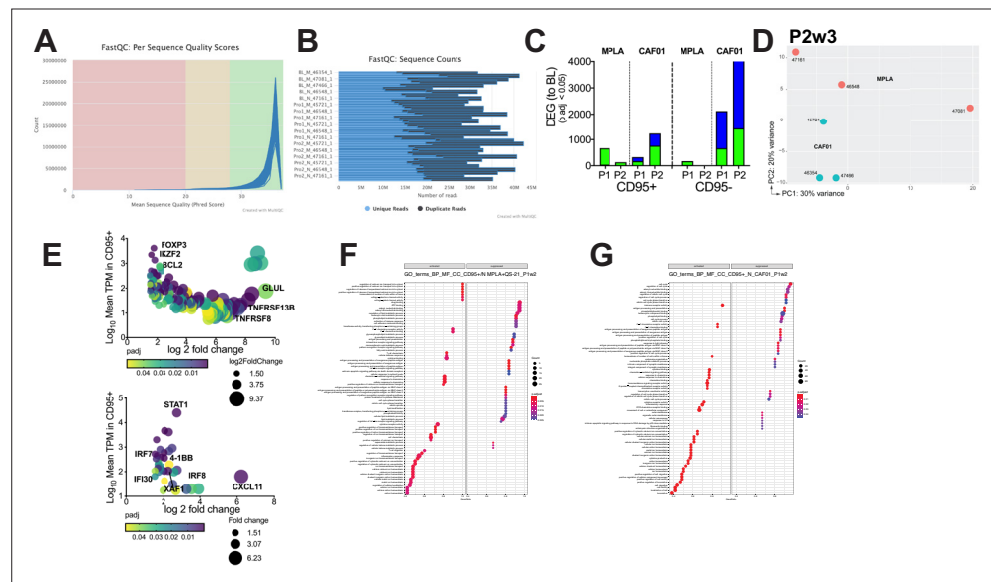


Figure 3—figure supplement 1. QC Metrics of RNA sequencing. (A–B) QC metrics (C) Bar graph shows DEG genes within CD4 subsets post vaccination relative to baseline. (D) PCA plot of CD95 +CD4 T cell subsets at P2w3 (E) Bubble plots show DEG enriched in CD95 +subsets at P1w2 in CAF01 and MPLA. GO-Terms of biological pathways differential induced in MPLA (F) and CAF01 (G) in CD95 +CD4 T cells at P1w2.

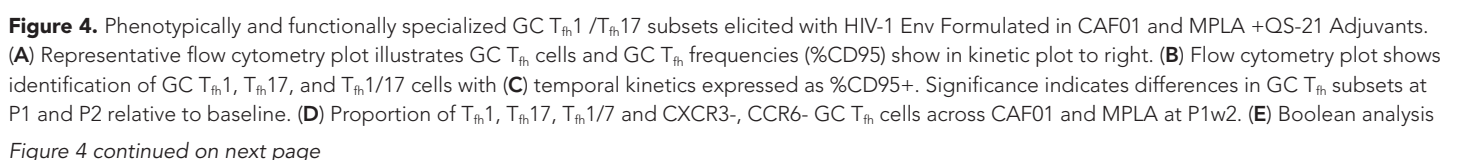


Figure 4 continued

(n=6 each group) shows proportion of T_{h1} , T_{h17} and $T_{h1/17}$ GC T_{fh} subsets. **(F–G)** Intracellular cytokine staining (ICS) analysis of T_{h1} , T_{h17} , $T_{h1/17}$ subsets at P1w2. **(H)** Gating strategy (left) and frequencies (right) of circulating T_{fh} (cT_{fh}) and cT_{fh1} cells in whole blood at P1w0 and P1w1. **(I)** Gating strategy (left) and frequencies (right) of activated ($CD40L^{+}OX40^{+}$) cT_{fh} ($CXCR5^{+}$) and non- cT_{fh} CD4 T cells ($CXCR5^{-}$) cells in PBMCs at P1w1. **(J)** ICS of cT_{fh} and non- cT_{fh} CD4 T cells following Env stimulation at P1w1 and P2w1. Data points show individual animals. Statistical analysis was performed using two-tailed Wilcoxon matched-pairs signed rank test (in panels **A**, **C**, **H**) or Mann-Whitney U test (in panels **D**; **G**, **I–K**); * $p < 0.05$, ** $p < 0.01$.

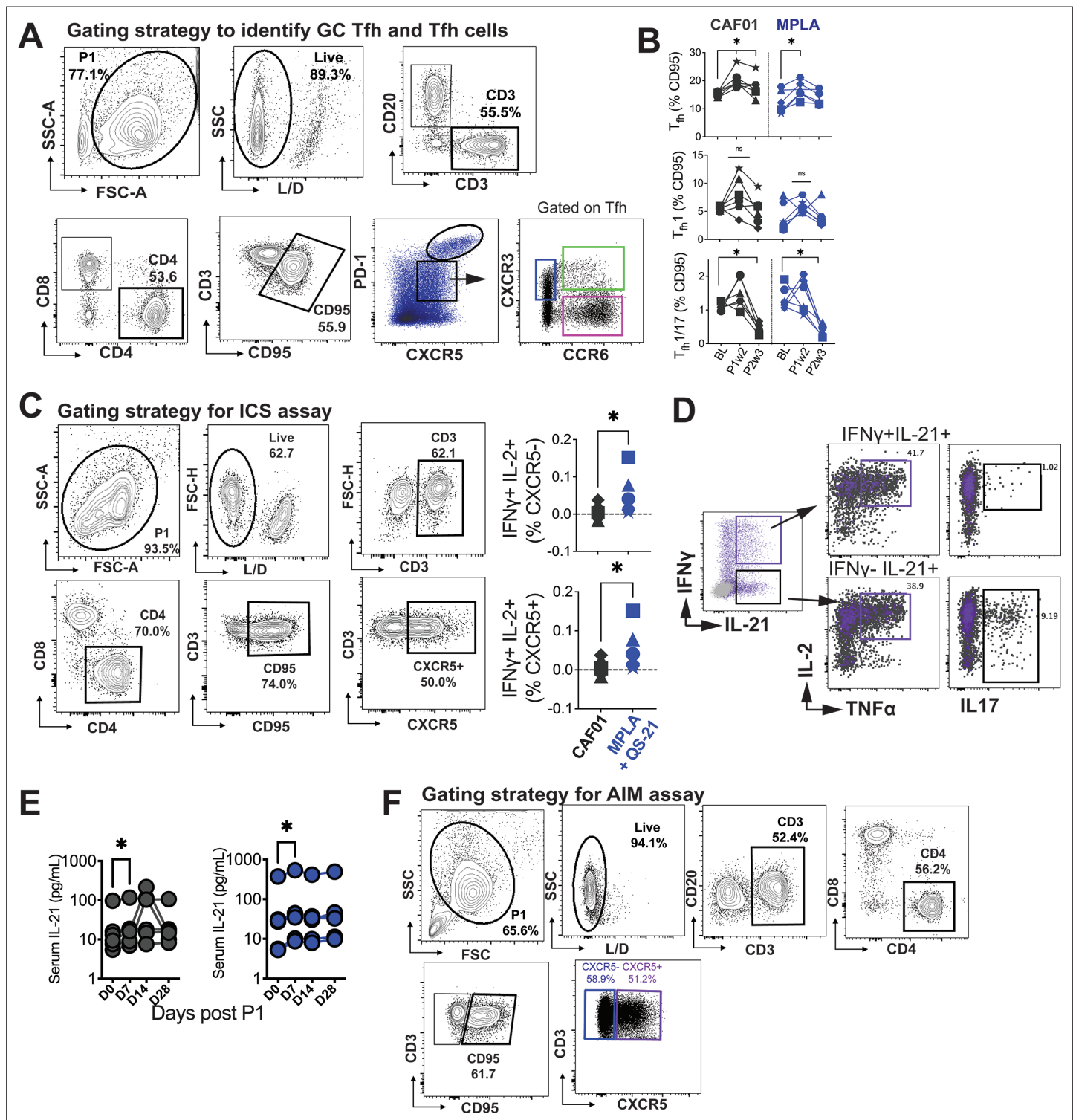


Figure 4—figure supplement 1. Gating strategy to identify GC T_{fh} and T_{fh} cells in lymph nodes. (A) Illustrates gating strategy to identify GC T_{fh} cells. (B) Frequencies of T_{fh} cells (CD4⁺CD95⁺PD-1⁺CXCR5⁺) (Top), T_{fh}1 cells (CD4⁺CD95⁺PD-1⁺CXCR5⁺CXCR3⁺) (Middle), and T_{fh}1/17 cells (CD4⁺CD95⁺PD-1⁺CXCR5⁺CXCR3⁺CCR6⁺) in lymph nodes. (C) Intracellular cytokine staining (ICS) to identify Env-specific T_{fh} cells. (D) Co-expression of IL-2 and TNFα in IFNγ⁺ versus IFNγ⁻ subsets producing IL-21. (E) Serum IL-21 post P1. (F) Gating of AIM assay.

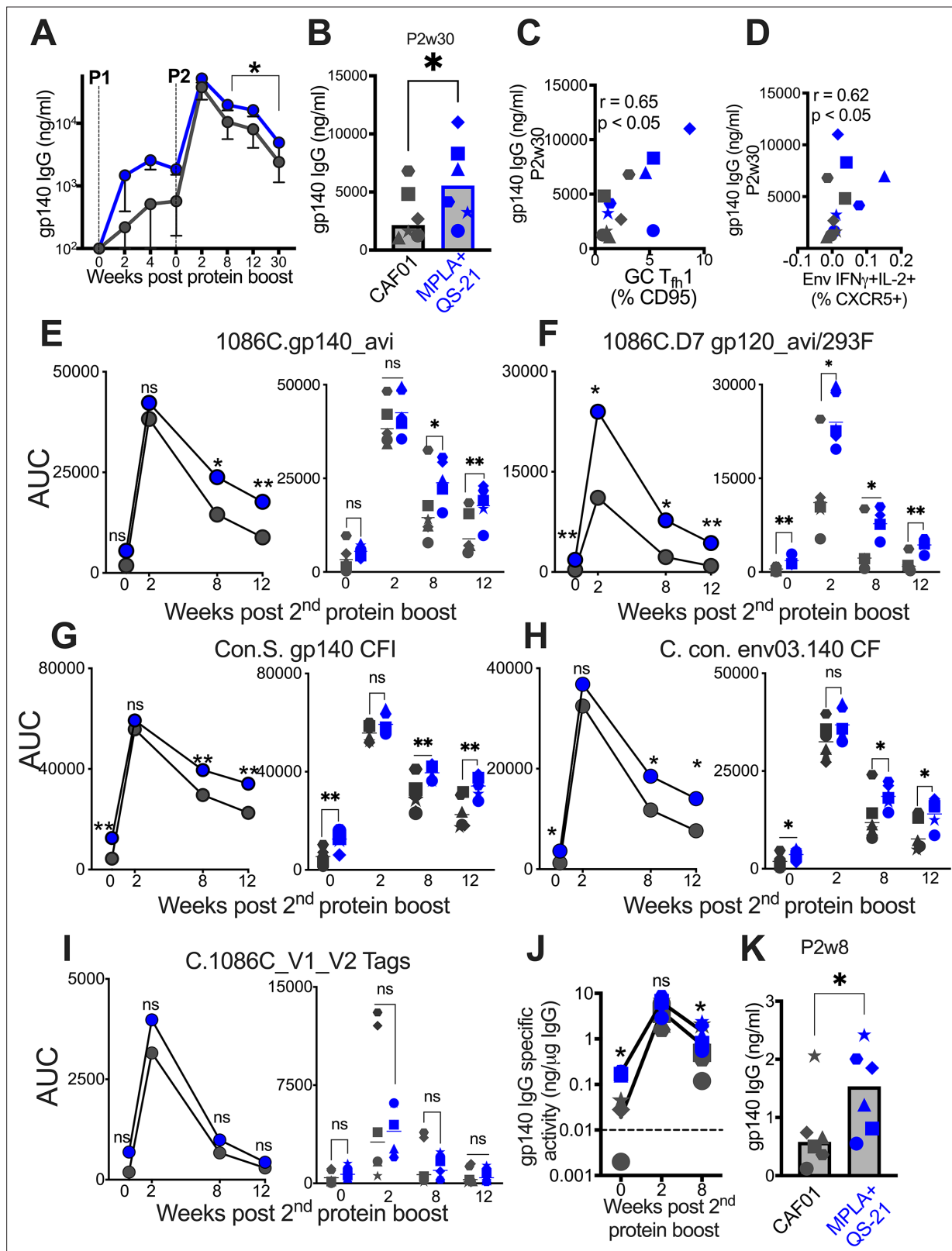


Figure 5. Induction of persistent anti-Env IgG antibodies with HIV-1 Env/MPLA + QS-21. (A) Kinetics of HIV-1 Env IgG post protein boost (P1 and P2) across vaccine regimens measured by ELISA against C. 1086 gp140. (B) Serum gp140 IgG week 30 post P2w3. (C) GC T_{H1} cells correlate with gp140 IgG at week 30. (D) Env-specific (IFN γ +IL-2 $^{+}$) T_{H1} cells correlate with gp140 IgG at week 30. (E–I) Area under the curve (AUC) values of IgG temporally shown by antigens, as indicated. (J) Temporal and (K) week 8 measures of gp140-specific IgG levels relative to total IgG in rectal secretions. Data points

Figure 5 continued on next page

Figure 5 continued

show individual animals. Statistical analysis was performed using Mann-Whitney U test (in panels **A-B**, **E-K**), or two-tailed Spearman rank correlation test (**C-D**); * $p < 0.05$, ** $p < 0.01$.

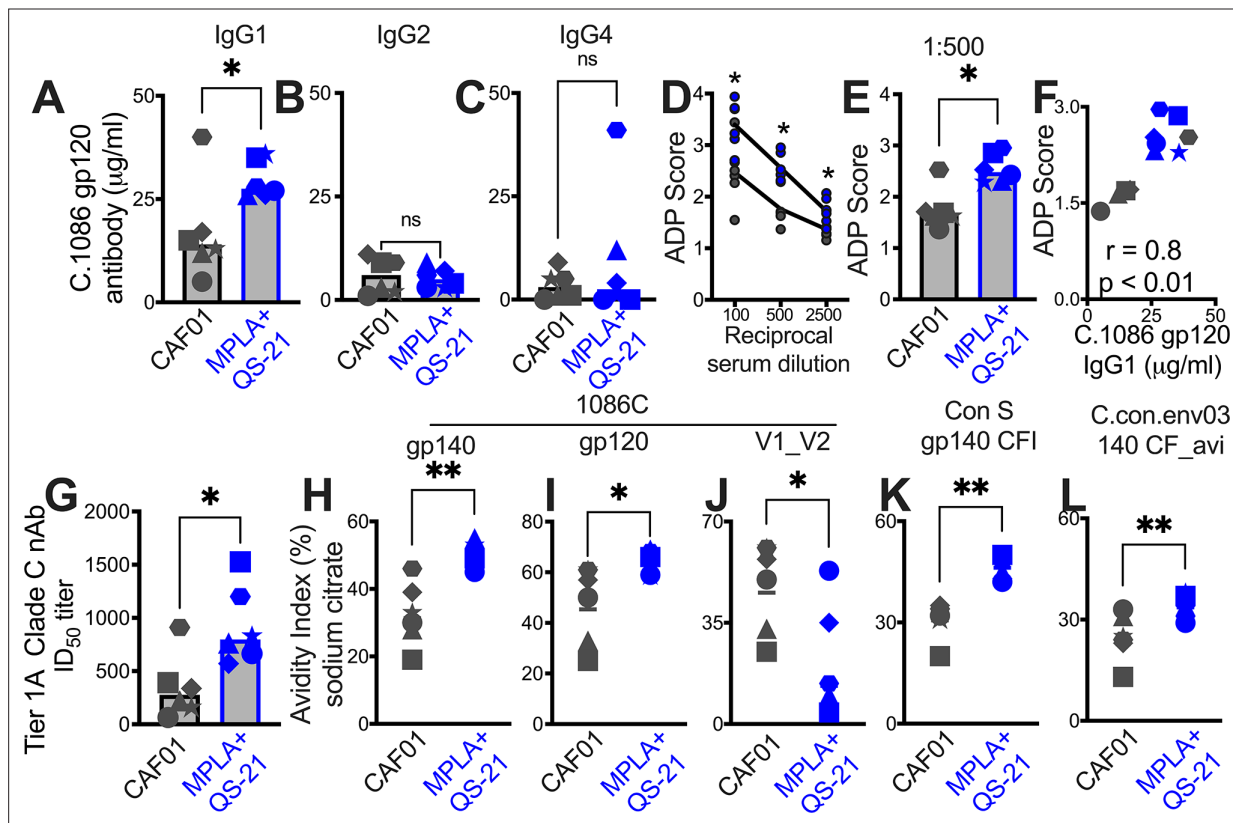


Figure 6. Induction of IgG1 subclass antibodies with greater effector functions with HIV-1 Env/MPLA +QS-21. Serum C. 1086 gp120-specific (A) IgG1, (B) IgG2 (C) IgG4 antibodies at P2w2. (D–E) Antibody-dependent phagocytosis (ADP) score at P2w8. (F) C. 1086 gp120-specific IgG1 correlates with ADP score. (G) Infectious dose 50% (ID₅₀) titers to Tier 1 A Clade C MW965.26 HIV-1 isolate at P2w2. (H–L) Avidity index (with sodium citrate) across vaccine regimens against specific antigens at P2w8. Data points show individual animals. Statistical analysis was performed using two-tailed Mann-Whitney U test (in panels A–E; G–L), or two-tailed Spearman rank correlation test (F); * p<0.05, **p<0.01.

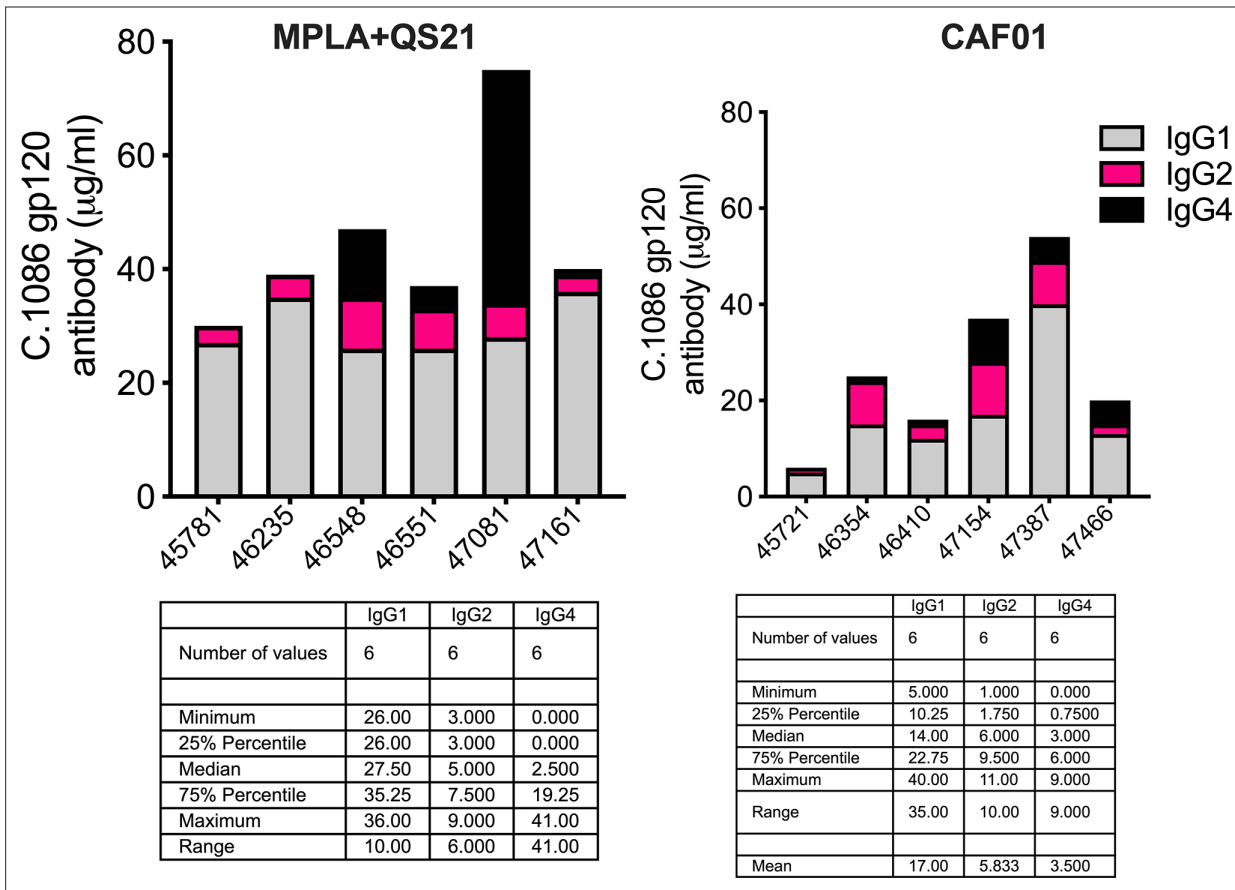


Figure 6—figure supplement 1. Serum C. 1086 gp120-specific IgG1 (grey), IgG2 (pink), and IgG4 (black) in animals (x-axis – animal IDs) P2w3.

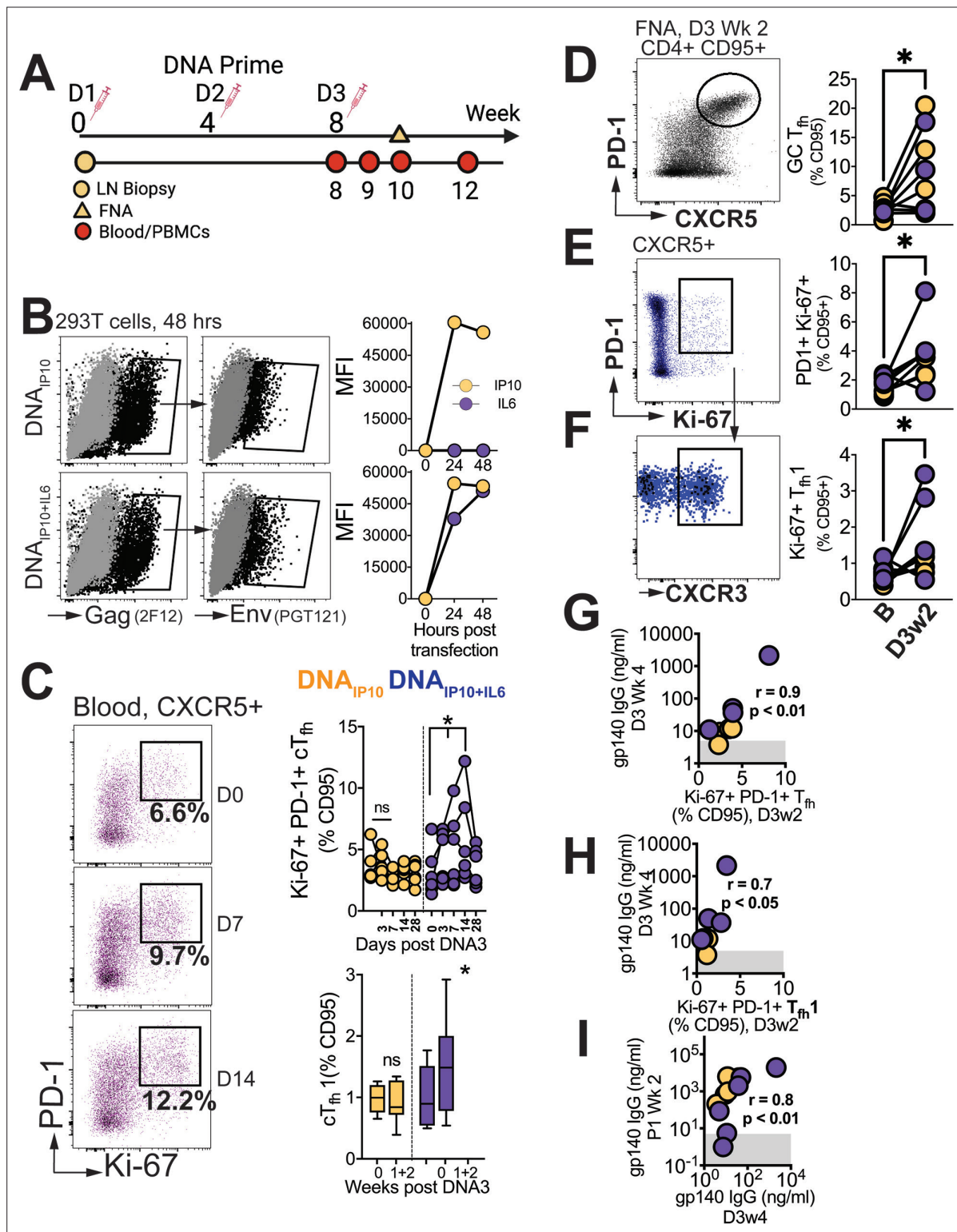


Figure 7. Differentiation of GC T_{fh} Subsets initiated during the DNA priming phase. **(A)** Experimental design of DNA immunization phase; FNA, lymph node fine needle aspirates. **(B)** Intracellular expression of Gag (2F12), surface expression of HIV-1 Env (PGT121) and IP10 and IL6 in supernatants of transfected 293T cells. **(C)** Flow cytometry plots show activated (PD-1⁺Ki-67⁺) cT_{fh} cells, frequencies post DNA3 (right top); frequencies of cT_{fh}1 cells (right bottom). **(D)** GC T_{fh} cells, **(E)** Ki-67⁺ PD-1⁺ cells of CXCR5⁺ subset in lymph node. **(F)** CXCR3⁺ subset of Ki-67⁺ PD-1⁺ CXCR5⁺ subset. **(G)** Ki-67⁺ PD-1⁺ T_{fh} in LN correlate with gp140 IgG at week 4 post DNA3. **(H)** Ki-67⁺ PD-1⁺ T_{fh} in LN correlate with gp140 IgG at week 4 post DNA. **(I)** gp140 IgG at week 2 post P1 correlates with gp140 IgG at week 4 post DNA3. Data points show individual animals. Statistical analysis was performed using one-tailed Wilcoxon matched-pairs signed rank test (in panels C-F), or Spearman rank correlation test (**G-I**); * p < 0.05.

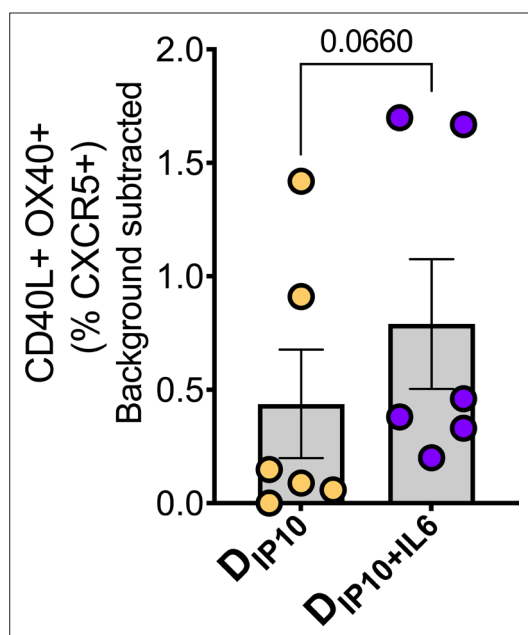


Figure 7—figure supplement 1. Frequencies of OX40⁺CD40L⁺ cTfh cells stimulated ex vivo with Gag and Env.